Journal of Advanced Research in Fluid Mechanics and Thermal Sciences

Journal homepage:
https://semarakilmu.com.my/journals/index.php/fluid_mechanics_thermal_sciences/index
ISSN: 2289-7879

Development of a Natural Draft Metal Biomass Cookstove for Community Kitchen

Sandeep Kore[1], Kailasnath Sutar[2,*], Akash Waghmare[1]

[1] Department of Mechanical Engineering, Vishwakarma Institute of Information Technology, Kondhwa (Budruk), Pune-411048, India
[2] Department of Mechanical Engineering, Bharati Vidyapeeth (Deemed to Be University) College of Engineering, Pune-Satara Road, Katraj, Pune-411043, India

ARTICLE INFO

Article history:
Received 13 August 2022
Received in revised form 15 December 2022
Accepted 26 December 2022
Available online 12 January 2023

Keywords:
Community cookstove; natural draft; input power; efficiency; fluid flow; heat transfer

ABSTRACT

Present work reports details of the design, fabrication, and laboratory testing of a natural draft metal biomass cookstove for a community kitchen. Heat transfer and fluid flow considerations along with experimental data available in the literature are used for the design of the community cookstove. The summation of pressure drop in different sections of the cookstove is compared with the outside pressure drop for the system using buoyancy considerations. The cookstove is fabricated as per the dimensions finalized during the design stage. Laboratory testing of the cookstove is conducted according to Bureau of Indian Standards (BIS) protocol. The tests are conducted under different conditions of main air hole closing viz. 0%, 25%, 75% and 100%. Each test is replicated thrice and an analysis of data is performed using a student's t-test. The efficiency of cookstove is found to be about 42% i.e., well above the BIS limit of 25% for natural draft metal cookstove. The effect of insulation on the outer body of cookstove is studied experimentally. It is found that the efficiency enhances by about 5.3% due to insulation. The authors found that provision of primary and secondary air holes play a very important role in the performance of the cookstove. When 100% main air holes are closed, the average efficiency of the cookstove is found to be poor (27.3%) due to no supply of secondary air to the combustion chamber of the cookstove.

1. Introduction

The early According to WHO [1], about 2.4 billion people across the globe use traditional biomass cookstoves using different types of biomasses such as wood, animal dung, crop waste, and coal as fuels. Each year about 3.2 million people die prematurely due to illnesses attributable to indoor air pollution. Indoor air pollution also causes diseases including stroke, heart disease, chronic obstructive pulmonary disease (COPD), and lung cancer. Close to half of deaths due to pneumonia among children under 5 years of age are caused by particulate matter (soot) inhaled from Indoor air pollution.

* *Corresponding author.*
E-mail address: kbsutar@bvucoep.edu.in

https://doi.org/10.37934/arfmts.102.2.120

For more than 3 decades, researchers across the world are performing research on clean cooking using biomass cookstoves. Report on the work done by various researchers in the form of design, development, laboratory and field testing, and dissemination of biomass cookstoves and discussion on various social issues related to the cookstoves is found in different review articles [2-13].

According to BIS protocol [14], solid biomass cookstoves having power output ratings in the range of 3 kW to 10 kW are known as community cookstoves. Such cookstoves are used by a group of people in community kitchens. Community cookstoves are used in schools, at religious places, in community gatherings, etc. for cooking food. Biomass cookstoves can be classified as natural draft and forced draft based on the draft created in the cookstove. Based on the methodology of air supplied to the cookstoves, they are classified as gasifier and combustion cookstoves. The cookstove in which solid biomass is converted into a combustible gaseous product by thermochemical conversion is known as a gasifier cookstove. The cookstove in which biomass burns completely in the stages of drying, pyrolysis, flaming combustion of pyrolysis products, and glowing combustion of char in presence of excess air, is known as a combustion cookstove [9]. In both gasifier and combustion cookstoves, the air is supplied in two parts *viz*. primary and secondary. In gasifier cookstoves, biomass is generally fed once whereas, in combustion cookstoves, biomass is fed continuously or in a batch.

The available literature focuses more on domestic cookstoves having a power output range of 2-5 kW. Very limited literature is available on the design and development of community cookstoves. Debajit and Sanjay [15] developed updraft and downdraft gasifier systems for community cooking. The authors reported a 65% saving in fuel as compared with traditional cooking systems. A report by Smokeless Cookstove Foundation [18] presents characteristics of different types of community cookstoves available in India. These cookstoves are Vikram Jumbo Chulha, Greenway Jumbo stove, Envirofit EFI-100L, Saverpro Aghanya stoves, TIDE Pyro stove, and Prakti Institutional stove. The information on cookstove manufacturer, efficiency, fuel burning, food cooking capacity, warranty, approximate cost, etc. is provided in the report. Robinson *et al.,* [19] reported results of a natural draft Top Lit Up Draft (TLUD) Institutional Improved Cookstove (IIC). The efficiency of the cookstove was up to 59% at an input power of 25.5 kW with very low CO emissions. Baharuddin *et al.,* [20] reported use of organic Rankine cycle based biomass carbonization system for conversion of thermal energy into electricity. Jankaew *et al.,* [21] reported experimental and computational studies on crude palm oil combustion. It was found that higher preheat temperature and pressure resulted into long, high temperature flame with larger penetration. Martin *et al.,* [22] reported a methodology to reduce potassium contents in a biomass fuel *viz.* empty oil palm fruit bunches to improve its heating value and overall utilization as a renewable energy source. Domestic stove was used for the experimental investigations. Balli *et al.,* [23] reported experimental studies on a prototype gas fired furnace for a pottery- ceramic industry. The prototype furnace was found to be energy efficient as well as less polluting as compared with the traditional gas fired furnace. It is found from the available literature that detailed design, development, and testing of community cookstoves are not reported. The present manuscript reports the step-by-step design procedure, fabrication, and testing of the community cookstove.

2. Design of the Cookstove

For the present design of the cookstove for a community kitchen, input power is considered to be10 kW and the lower calorific value of biomass fuel was taken as 16 MJ/kg. The fuel burning rate for this combination comes out to be 37.5 g/min. One kilogram of biomass requires approximately 6 kilograms of air for complete combustion in ideal conditions. While designing a thermal system using solid fuel, 20% excess air is considered for complete combustion of the fuel. Hence, for the present case of a community cookstove, the amount of air requires comes out to be 37.5 × 6 × 1.2 = 270 g/min. Now, 70% of the required air is supplied near the base of the combustion chamber of the cookstove as a primary air for initiation of combustion, pyrolysis, oxidation, and char burning. The reaming 30% of the required air is supplied near the top of the combustion chamber as secondary air to burn the pyrolysis products so that the products of incomplete combustion shall be reduced and clean combustion is ensured.

The air enters from the holes provided near the lower portion of the outer body of the cookstove. Now, out of this total air, 70% of the primary air comes into the lower portion of the combustion chamber through the holes provided in the grate, and the remaining 30% is directed through the annular space between the combustion chamber and the outer body in the upward direction and enters into the combustion chamber through the secondary air holes near the top.

Figure 1 presents the schematic diagram of the proposed community cookstove with a pot shield. To calculate the number of primary and secondary air holes, the system of cookstove is divided into four zones. The calculations for pressure drop through these zones are performed considering basic concepts of fluid flow and heat transfer.

Bryden *et al.,* [24] reported design principles for biomass cookstoves. The authors have used these principles in deciding the dimensions of the proposed community cookstove. A detailed step-by-step procedure used for the calculation of a number of primary and secondary air holes for a given size of the holes and other dimensions of the cookstove is reported in this section.

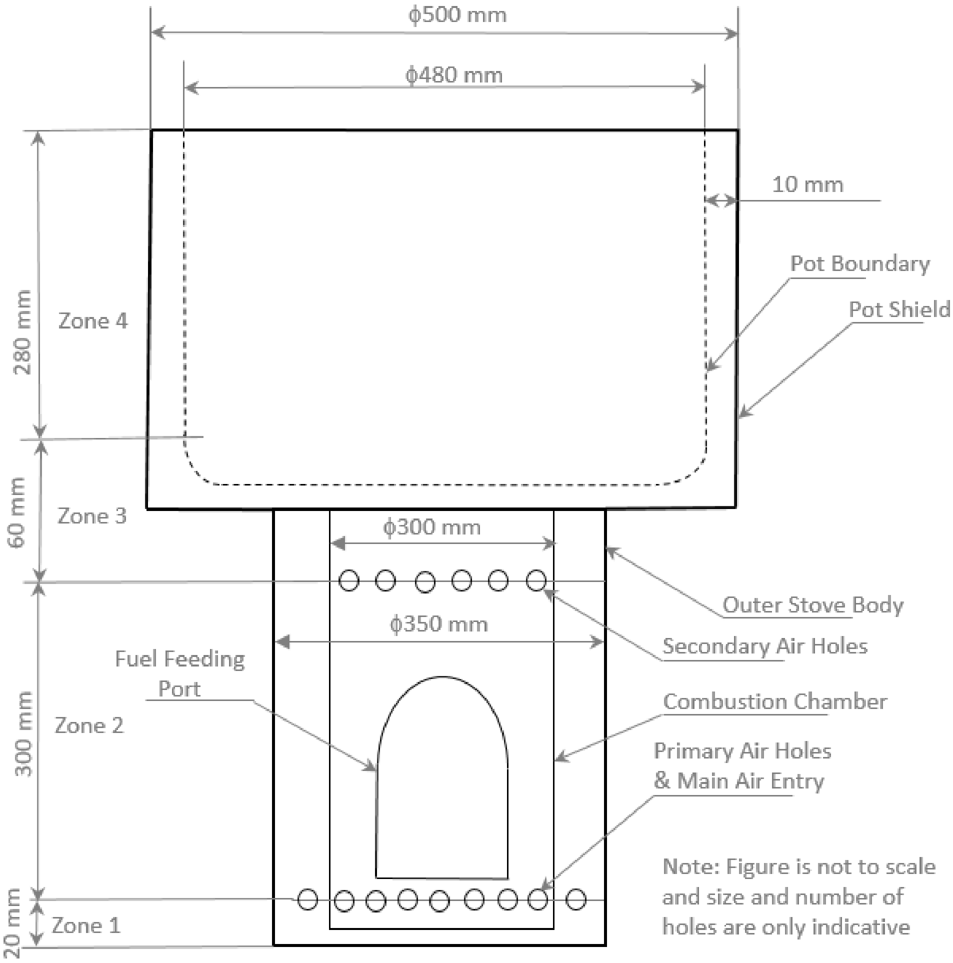

Fig. 1. Schematic diagram of proposed community cookstove

Table 1 reports the design parameters for proposed community cookstove.

Table 1
Design parameters for the proposed community cookstove

Parameter	Dimension
Diameter of combustion chamber	300 mm
Diameter of outer cylinder	350 mm
Diameter of main air entry holes on outer cylinder	14 mm
Diameter of primary and secondary air supply hole	14 mm
Number of main air entry holes on outer cylinder	20
Number of primary air entry holes	14 (Assumed)
Number of secondary air entry holes	06 (Assumed)
Height of combustion chamber	360 mm

To start with design of the proposed community cookstove, consider,

Input power of a community cookstove: 10 kW

Lower calorific value of a biomass fuel: 16 MJ/kg

Fuel burning rate of cookstove: 10 kJ/s/(16000 kJ/kg) = 0.000625 kg/s = 0.625 g/s = 37.5 g/min

Stoichiometric air fuel ratio: 6:1

Considering 20% excess air, actual air fuel ratio: 7.2:1

That is, 1 gram of fuel requires 7.2 grams of air or 37.5 grams of fuel requires 270 grams of air

Amount of primary air: $\dot{m}_{pa}$ = 70% of 270 grams = 189 g/min = 0.00315 kg/s

Amount of secondary air: $\dot{m}_{sa}$ = 30% of 270 grams = 81 g/min = 0.00135 kg/s

Amount of total air $\dot{m}_t = \dot{m}_{pa} + \dot{m}_{sa} = 0.0045$ kg/s

2.1 Outside Pressure Drop ($\Delta P_{outside}$)

The total height between centre of main air entry air holes on outer cylinder and the topmost point of the cookstove i.e., H = 640 mm.

Hence, outside pressure drop between points A and B due to difference in elevation [25]:

$$\Delta P_{outside} = \rho_a \times g \times H = 1.165 \times 9.81 \times 0.640 = 7.314 \text{ N/m}^2 \text{ or Pa} \quad (1)$$

where, ρ: density of air in kg/m^3. At ambient temperature of 30 ^oC, ρ_a = 1.165 kg/m^3.

2.2 Inside Pressure Drop (ΔP_{inside})

During travel of primary and secondary air through the cookstove, a pressure drop occurs at different locations such as entry of primary and secondary air holes, porous bed of biomass, annular space between the combustion chamber and the outer body, annular space between the pot and shield, etc. The summation of all these pressure drops is accounted for in the calculations for the inside pressure drop.

For calculation of inside pressure drop, the system of cookstove is divided into four zones *viz.* zone 1, 2, 3 and 4.

For creating a natural drat of air through the cookstove, the inside pressure drop must be less than or equal to the outside pressure drop between the entry at zone 1 and the exit at zone 4.

2.2.1 Pressure drop in zone 1

It includes pressure drop through main air entry holes (ΔP_{ma}) through primary air entry holes (ΔP_{pa}) and also through grate (ΔP_{grate}).

<u>Pressure drop through main air entry holes (ΔP_{ma})</u>

Air enters through main air entry holes at ambient temperature of 30 ^{0}C, ρ_a = 1.165 kg/m^3
Diameter of each hole = 14 mm and number of holes = 20
Total area of main air entry holes, $A_{ma} = (\pi /4) \times (0.014)^2 \times 20 = 0.003078761$ m^2

Let us assume that all the air required for complete combustion of fuel enters through these holes only.

Hence, velocity of air at inlet of main air holes, $V_{ma} = \dot{m}_t/(\rho_a \times A_{ma}) = 0.0045/(1.165 \times 0.003078) =$ 1.255 m/s

Pressure drop at inlet of main air holes,

$$\Delta P_{ma} = 0.5 \times \rho_a \times V_{ma}^2 = \underline{0.91745\text{ Pa}} \tag{2}$$

<u>Pressure drop through primary air entry holes (ΔP_{pa})</u>

Air enters through primary air entry holes at ambient temperature of 30 ^{0}C, ρ_a = 1.165 kg/m^3
Diameter of each hole = 14 mm and number of primary air entry holes = 14
Total area of primary air entry holes = $A_{pa} = (\pi /4) \times (0.014)^2 \times 14 = 0.002155$ m^2

It is assumed that 70% of the primary air required for pyrolysis and oxidation of fuel enters through these holes only.

Hence, velocity of air at inlet of primary air holes, $V_{PA} = \dot{m}_{pa}/(\rho_a \times A_{pa}) = 0.00315/(1.165 \times 0.002155)$ = 1.2547 m/s.

Pressure drop at inlet of primary air holes,

$$\Delta P_{pa} = 0.5 \times \rho_a \times V_{pa}^2 = \underline{0.91701\text{ Pa}} \tag{3}$$

<u>Pressure drop through grate (ΔP_{grate})</u>

The whole primary air supplied to the cookstove enters into the combustion chamber through grate. The grate is a plate of 2 mm thickness with diameter of 300 mm. 120 holes of 8 mm diameter are drilled in the plate to allow entry of the primary air into the combustion chamber. Assuming temperature of primary air entering through the grate into the combustion chamber to be 30 ^{o}C, its density will be ρ_a = 1.165 kg/m^3.

Total area of holes in the grate = A_{grate} = (π /4) × (0.008)^2 × 120 = 0.754 m^2.

Hence, velocity of air at the inlet of holes in the grate, $V_{grate} = \dot{m}_{pa}/(\rho_a \times A_{grate})$ = 0.00315/(1.165 × 0.754) = 0.00359 m/s.

Pressure drop at inlet of holes in the grate,

$\Delta P_{grate} = 0.5 \times \rho_a \times V_{grate}^2 \approx$ <u>0.00 Pa</u> (4)

2.2.2 Pressure drop in zone 2

It includes pressure drop through porous bed of fuel (ΔP_{bed}) as well as during flow of secondary air through annular space between the combustion chamber and outer cylinder (ΔP_{as}).

<u>Pressure drop through porous bed of fuel (ΔP_{bed})</u>

Gudekote and Choudhari [26] reported the effect of velocity slip and the angle of inclination on the motion of casson fluid flowing through an elastic tube with porous walls. The authors found that with increase in porosity there was significant decrease in pressure drop.

Height of porous fuel bed, h_{bed} = 300 mm and diameter of combustion chamber = 300 mm

Temperature of combustion chamber is taken as 800^{o}C from the data available in the research by Brady *et al.,* [27].

Considering the fluid to be the wood gas, at T_g = 1073 K, different properties of wood gas available in a research by MacCarty and Bryden [28] are:

$\mu_g = (-7 \times 10^{-12}\, T^2 + 4 \times 10^{-8}\, T + 8 \times 10^{-6})$ kg/m-sec = 4.2861 × 10^{-5} kg/m-sec,

ρ_g = (353.09/T) kg/m^3 = 0·32907 kg/m^3

Cross-sectional area of the combustion chamber, A_{cc} = (π/4) × (0.03)^2 = 0.07069 m^2

Mass flow rate of fluid through combustion chamber m_{cc} = mass flow rate of fuel (m_f) + mass flow rate of primary air ($\dot{m}_{pa}$)

$\dot{m}_{cc}$ = 37.5 g/min + 189 g/min = 226.65 g/min = 0.003775 kg/sec

Hence, velocity of hot air in porous bed, $V_{bed} = \dot{m}_{cc}/(\rho_a \times A_{cc})$ = 0·16202 m/sec.

Pressure drop due to flow of fluid through porous bed of biomass particles is calculated using Ergun relation reported by Kaviany [29].

$$\Delta P_{bed} = \left\{\frac{\alpha\, \rho_g\, V_{bed}{}^2\, h_{bed}\, (1-\varepsilon_{bed})^2}{\varepsilon_{bed}{}^3\, d_{c,bp} Re_{bp}}\right\} + \left\{\frac{\beta\, \rho_g\, V_{bed}{}^2\, h_{bed}\, (1-\varepsilon_{bed})}{\varepsilon_{bed}{}^3\, d_{c,bp}}\right\} \tag{5}$$

where, α = 180; β = 4 (for rough biomass particles); ε_{bed} is bed porosity = 0.5 (assumed); V_{bed}: Velocity of fluid in reactor, Reynolds number of biomass particles, $Re_{bp} = \frac{\rho_g\, V_{bp}\, d_{c,bp}}{\mu_g}$; characteristic particle diameter $d_{c,bp}$ = 6/Ao where, Ao = surface area of particle/volume of particle. For average particle diameter of 20 mm and height of 30 mm, A_o comes out to be 266.67 m^{-1}. Hence, $d_{c,bp}$ = 6/Ao = 0.0225 m.

$$Re_{bp} = \frac{\rho_g\, V_{bed}\, d_{c,bp}}{\mu_g} = \frac{0.32907 \times 0.16202 \times 0.0225}{4.2861 \times 10^{-5}} = 27.9883 \tag{6}$$

Substituting all value in Eq. (4), pressure drop through porous bed of biomass particles

ΔP_{bed} = {((180 × 0.32907 × $(0.16202)^2$ × 0.3 × $(1 - 0.5)^2$))/(0.5^3 × 0.0225 × 27.9883)} + {((4 × 0.32907 × $(0.16202)^2$ × 0.3 × (0.5)))/(0.5^3 × 0.0225)} = 1.4815 + 1.8428 = <u>3.3243</u> Pa

<u>Pressure drop during flow of secondary air through annular space</u> (ΔP_{as})

The secondary air passing through the annular space between the combustion chamber and outer cylinder gets heated due to convective and radiative heat transfer. The temperature of gases inside the combustion chamber is taken from the literature is 1073 K [27].

Zube [30] reported that in case of a natural draft biomass cookstove with a pot shield, total convective and radiative losses between the combustion chamber and the side wall are about 5.6% and 15.5% respectively of the total energy produced by combustion of wood.

Now, for the given design of cookstove with 10 kW_{th} input power,

Rate of heat lost to the wall of the combustion chamber by convection, $\dot{Q}_{conv}$ = 560 W

Rate of heat lost to the wall of the combustion chamber by radiation, $\dot{Q}_{rad}$ = 1550 W

Total rate of heat lost to the wall of combustion chamber ($\dot{Q}_{lost}$) = Heat lost by convection ($\dot{Q}_{conv}$) + Heat lost by radiation ($\dot{Q}_{rad}$) = Heat transfer by conduction through wall of combustion chamber ($\dot{Q}_{cond,cc}$) = Heat lost by convection through outside of combustion chamber to the secondary air flowing through the annular space between the combustion chamber and the outer wall ($\dot{Q}_{conv,as}$)

$$\dot{Q}_{lost} = \dot{Q}_{conv} + \dot{Q}_{rad} = \dot{Q}_{cond,cc} = \dot{Q}_{conv,as} = 2110\ \text{W} \tag{7}$$

Now, $\dot{Q}_{conv}$ = 560 W = $h_{conv,cc}$ × A_{surf} × (T_g - $T_{cc,is}$) (8)

where, Convective heat transfer coefficient, $h_{conv,cc}$ = 10 W/m^2K [28]

Inner surface area of the combustion chamber, A_{surf} = π × $D_{i,cc}$ × h_{cc} = 0.28274 m^2

Inner diameter of the combustion chamber, $D_{i,cc}$ is 300 mm

Height of combustion chamber, h_{cc} is 300 mm

Then, temperature of inner surface of the combustion chamber $T_{cc,is}$ is found to be 874.94 K.

Now, with this value of $T_{cc,is}$, radiative heat transfer coefficient ($h_{rad,cc}$) shall be estimated.

For $\dot{Q}_{rad}$ = 1550 W = $h_{rad,cc} \times A_{surf} \times (T_g - T_{cc,is})$, $h_{rad,cc}$ = 27.68 W/m^{2}K (9)

For conduction heat transfer through cross section of the combustion chamber of 2 mm thickness,

$$\dot{Q}_{lost} = \dot{Q}_{cond,cc} = \frac{(T_{cc,is} - T_{cc,os})}{\left(\frac{\ln\left(R_{i,ob}/R_{o,cc}\right)}{2\pi k_{cc} h_{cc}}\right)} \quad (10)$$

Using Eq. (9), the unknown temperature at the outer surface of the combustion chamber i.e., $T_{cc,os}$ is calculated, which is found to be 871.351 K or 598.351^{o}C (Figure 2).

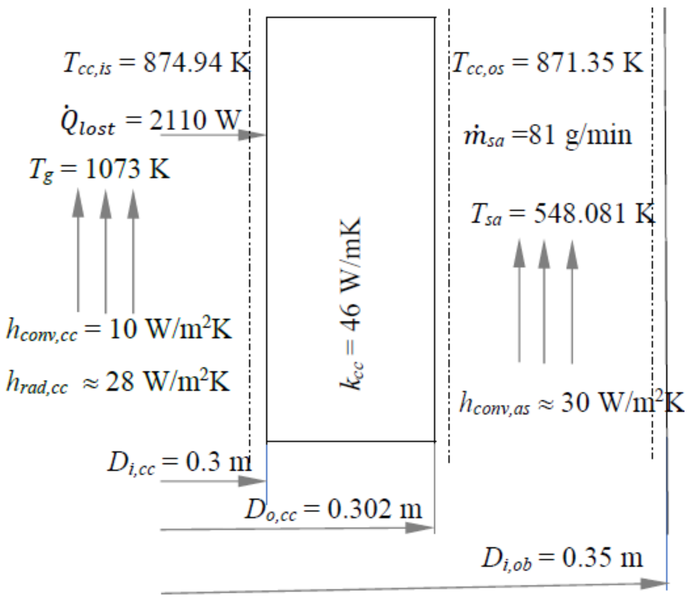

Fig. 2. Fluid flow and heat transfer through combustion chamber

Assuming the overall heat transfer coefficient at the interface of outer surface of combustion chamber and the flow of secondary air, *i. e.* $h_{cc,as}$ = 30 W/m^{2}K, average temperature of the secondary air (T_{sa}) in the annular space between the combustion chamber and the outer body can be estimated.

For uniform surface temperature condition, for estimation of convective heat transfer through annular space between the combustion chamber and the outer body, following relations is suggested by Bergman *et al.,* [31]

$\dot{Q}_{conv,as} = h_{conv,as} \times A_{cc,os} \times \Delta T_{lm}$ = 2110 W (11) where, log mean temperature difference ΔT_{lm} is given as

$$\Delta T_{lm} = \frac{(T_{cc,os}-T_{sa,2})-(T_{cc,os}-T_{sa,1})}{ln\left(\frac{(T_{cc,os}-T_{sa,2})}{(T_{cc,os}-T_{sa,1})}\right)} \quad (12)$$

In Eq. (10), outside surface area of combustion chamber, $A_{cc,os} = \pi \times D_{o,cc} \times h_{cc}$ = 0.28463 m^2 and overall heat transfer coefficient, $h_{cc,as}$ = 30 W/m^{2}K. The temperature of outside surface of combustion chamber ($T_{cc,os}$) is assumed to be constant at steady state and its value is found to be 871.351 K from Eq. (9). The temperature of secondary air at the inlet of the annular space ($T_{sa,1}$) is 303 K and that at the outlet of the annular space ($T_{sa,2}$) is found to be 793.162 K from Eq. (11). Then the average temperature of the secondary air, $T_{sa} = (T_{sa,1} + T_{sa,2})/2$ is found to be 548.081 K or 275.081^{o}C.

Now, to calculate pressure drop during flow of secondary air through annular space i.e., ΔP_{as}, the properties of air at 548.081 K are found to be: ρ_{sa} = 0.629039 kg/m^3, μ_{sa} = 2.85605 × 10^{-5} kg/m-s.

Velocity of secondary air flowing through the annular space between combustion chamber and the outer body of the stove is given by,

$v_{sa} = \dot{m}_{sa} /(\rho_{sa} \times A_{as})$; where, the area of annular space, $A_{as} = \pi\ (D_{i,ob}^2 - D_{o,cc}^2)/4$ (13)

where, $D_{i,ob}$: Inner diameter of outer body and $D_{o,cc}$: Outer diameter of combustion chamber.

Then, A_{as} = 0.02458 m^2 also, $\dot{m}_{sa}$ = 0.00135 kg/s, then, v_{sa} = 0.00135/(0.629039 × 0.02458) = 0.087313 m/s.

At this velocity of secondary air, Reynold's number of the flow is given by,

$Re = [\rho_{sa} \times v_{sa} \times D_{as}]/\mu_{sa}$ (14)

Now, Re_{sa} = (0.629039 × 0.087313 × 0.326)/ (2.85605 × 10^{-5}) = 626.912

As Reynold's number is less than 2300, the flow is laminar. Hence, Darcy friction factor (f) can be calculated as [31]:

$f = 64/Re$ = 64/626.9012 = 0.1021 (15)

Now, $\Delta P_{as} = (\rho_{sa} \times f \times h_{cc} \times v_{sa}^2)/(2D_{as})$ = <u>0.000225</u> Pa (16)

2.2.3 Pressure drop in zone 3

It includes pressure drop at secondary air inlet into combustion chamber through holes (ΔP_{sa}) and also pressure drop due to 90^o bend/tilting of burnt gases at two places (ΔP_{bend}).

<u>Pressure drop at secondary air inlet into combustion chamber through holes (ΔP_{sa})</u>

Number of secondary air holes = 06 and diameter of each hole = 14 mm

Total area of secondary air entry holes = $A_{sa,h}$ = (π /4) × (0.014)^2 × 06 = 0.000924 m^2

Then, velocity of secondary air at the entry to the holes, $v_{sa,h} = \dot{m}_{sa} /(\rho_{sa} \times A_{sa,h})$ = 2.3236 m/s

Hence, pressure drop at inlet of secondary air holes,

ΔP_{sa} = ($\rho_{sa} \times V_{sa,h}^2$)/2 = <u>1.69813</u> Pa (17)

<u>Pressure drop due to 90^o bend of burnt gases at two places (ΔP_{bend}):</u>

Mass flow rate of burnt gases $\dot{m}_g = \dot{m}_f + \dot{m}_{pa} + \dot{m}_{sa}$ = 0.005125 kg/s (18)

Zube [30] reported 819 K as temperature of flame near the pot bottom. Considering temperature of burnt gases T_g = 819 K near the pot bottom, properties of burnt gases [28],

$\mu_g = (-7 \times 10^{-12} T_g^2 + 4 \times 10^{-8} T_g + 8 \times 10^{-6})$ kg/m-sec = 3.60647×10^{-5} kg/m-sec,
$\rho_g = (353.09/T_g)$ kg/m^3 = 0·4311 kg/m^3

Now, velocity of burnt gases $v_g = \dot{m}_g/[\rho_g \pi(D_{shield}^2 - D_{pot}^2)/4]$ = 0.7723 m/s

$\Delta P_{bend} = k_{bend} \times \frac{(\rho_g \times v_g^2)}{2} = 0.95 \times \frac{(0.4311 \times 0.7723^2)}{2}$ = <u>0.1221</u> Pa (19)

where, K_{bend} = 0.95 [32].

Total pressure drop in two bens, ΔP_{bend} = 2 × 0.1221 Pa = <u>0.2442</u> Pa

2.2.4 Pressure drop in zone 4

It includes pressure drop in the annular space between the pot and the pot shield or skirt (ΔP_{shield}). Zube [30] reported a convective heat transfer coefficient of 14 W/m^{2}K for a shield gap of 10 mm in case of a natural draft metal cookstove. The author also reported that out of the total rate of heat gained by the pot, 55% is accounted by convective gain and 45% is accounted by radiative gain. Also, out of this rate of heat gain, about 21% of the radiative rate of heat gain and 65% of the convective rate of heat gain occurs from the pot shield.

Let us use above data for the present case of community cookstove with 10 kW input power. Assuming overall efficiency of the cookstove to be 35% i.e., net rate of heat gained by the pot will be 3.5 kW. Out of this total rate of heat gained by the pot, 45% i.e., 1575 W of energy will be coming through radiation and 55% i.e., 1925 W of energy will be received through convective rate of heat transfer. Now, Radiative and convective rate of heat gained by the pot from the burnt gases flowing through the gap between the pot and the shield will be 330.75 W (i.e., 21% of 1575 W) and 1251.25 W (i.e., 65% of 1925 W). Total rate of heat gained by the pot through shield will be 1582 W.

This rate of heat gained (1582 W) is used to heat water in the pot from about 25 ^{o}C to 95 ^{o}C along radial direction. Heat transfer coefficient for natural convection heating of water varies from 100 W/m^{2}K to 1200 W/m^{2}K [33]. Let, the average value of heat transfer coefficient on water side (h_{water}) be 650 W/m^{2}K. From this data, temperature of inner surface of aluminium pot ($T_{pot,is}$) is estimated as follows

$\dot{Q}_{gain} = h_{water} \times A_{pot,is} \times (T_{pot,is} - T_{water})$ = 1582 W (20) where, inner surface area of pot $A_{pot,is} = \pi \times D_{pot,is} \times h_{pot} = \pi \times 0.474 \times 0.28 = 0.417$ m^2 and $T_{water} = 95$ ^oC. From this data, $T_{pot,is}$ is found to be 373.837 K or 100.837 ^oC (Figure 3).

Now, considering conductive heat transfer from outer surface of aluminium to the inner surface along the radial direction, the temperature of outer surface of aluminium pot ($T_{pot,o}$) can be estimated.

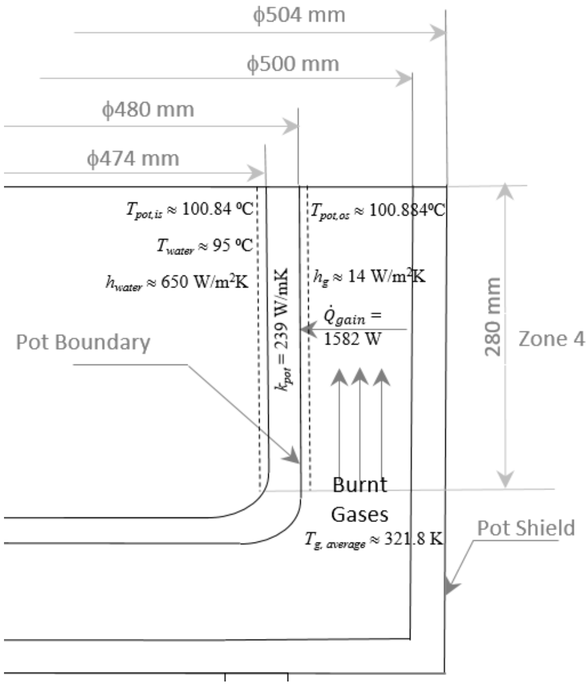

Fig. 3. Heat transfer and fluid flow in zone 4

For conduction heat transfer through cross section of aluminium pot of 3 mm thickness,

$$\dot{Q}_{gain} = \dot{Q}_{cond,pot} = 1582\ \text{W} = \frac{(T_{pot,os} - T_{pot,is})}{\left(\frac{\ln\left(R_{pot,os}/R_{pot,is}\right)}{2\pi k_{pot} h_{pot}}\right)} \tag{21}$$

where, $R_{pot,os} = 0.24$ m, $R_{pot,is} = 0.237$ m, $k_{pot} = 239$ W/mK, $h_{pot} = 0.28$ m. Using Eq. (21), the unknown temperature at the outer surface of the pot i.e., $T_{pot,os}$ is calculated, which is found to be 373.884 K or 100.884^oC [34].

Assuming the overall heat transfer coefficient at the interface of outer surface of the pot and the flow of burnt gases, i.e., $h_g = 14$ W/m^{2}K, temperature of the burnt gases ($T_{g,2}$) near exit of the annular space between the pot and the pot shield can be estimated.

$$\dot{Q}_{gain} = \dot{Q}_{conv,pot-skirt} = h_g \times A_{pot,os} \times ((T_{g,2} - T_{pot,os})) = 1582\ \text{W} \tag{22}$$

In Eq. (22), outside surface area of the pot, $A_{pot,os} = \pi \times D_{pot,os} \times h_{pot} = 0.42223$ m^2 and heat transfer coefficient on burnt gas side, $h_g = 14$ W/m^{2}K. The temperature of outside surface of the pot ($T_{pot,os}$) is assumed to be constant at steady state and its value is found to be 373.884 K from Eq. (21). Using Eq. (22), temperature of the burnt gases near the exit of the zone 4 ($T_{g,2}$) is found to be 641.5106 K.

Now, temperature of the burnt gases near the entry of the zone 4 ($T_{g,1}$) is 819 K. Then the average temperature of the burnt gases, $T_{g,average} = (T_{g,1} + T_{g,2})/2$ is found to be 594.796 K or 321.796 ^oC.

Now, to calculate pressure drop during flow of the burnt gases through annular space between the pot and the shield i.e., ΔP_{shield}, the properties of burnt gases at 594.796 K are found using following relationships:

$\mu_{g,shield}$ = (-7×10^{-12} $T_{g,average}{}^{2}$ + 4×10^{-8} $T_{g,average}$ + 8×10^{-6}) kg/m-sec = 2.93154×10^{-5} kg/m-sec, $\rho_{g,shield}$ = (353.09/$T_{g,average}$) kg/m^3 = 0·594 kg/m^3

Now, velocity of burnt gases flowing through the annular space between the outer surface of the pot and the shield of the stove is given by,

$$v_{g,shield} = \dot{m}_g/(\rho_{g,shield} \times A_{shield}) \tag{23}$$

where, the area of annular space, $A_{shield} = \pi(D_{pot,os}{}^{2} - D_{shiels,is}{}^{2})/4$ (24)

Here, $D_{pot,os}$: Outer diameter of the pot = 480 mm and $D_{shield,is}$: Inner diameter of the pot shield = 500 mm. Then, A_{shield} = 0.015394 m^2 also, $\dot{m}_g$ = 0.005125 kg/s, then, v_{shield} = 0.5605 m/s.

At this velocity of the burnt gases, Reynold's number of the flow is given by,

$$Re = [\rho_{g,shield} \times v_{g,shield} \times D_{shield,average}]/\mu_{g,shield} \tag{25}$$

where, average diameter at the shield, $D_{shield,average}$ = 490 mm. Now, Re_{sa} = (0.594 × 0.5605 × 0.49)/ (2.93154 × 10^{-5}) = 5564.96

As Reynold's number is greater than 2300, the flow is turbulent. Hence, Darcy friction factor (f) can be calculated as [31]:

$$f = (0.790 \times \ln Re - 1.64)^{-2} = [0.790 \times \ln(5564.96) - 1.64]^{-2} = 0.0374 \tag{26}$$

Hence, $\Delta P_{shield} = (\rho_{shield} \times f \times h_{pot} \times v_{shield}{}^{2})/(2 \times D_{shield,average}) = \underline{0.001994}$ Pa (27)

Now, total pressure drop in all four zones from Eq. (2), Eq. (3), Eq. (4), Eq. (15), Eq. (16), Eq. (18) and Eq. (26),

$\Delta P_{inside} = \Delta P_{ma} + \Delta P_{pa} + \Delta P_{bed} + \Delta P_{as} + \Delta P_{sa} + \Delta P_{bend} + \Delta P_{shield}$ = 0.91745 + 0.91701 + 3.3243 + 0.000225 + 1.69813 + 0.1221 + 0.001994 = $\underline{6.981209}$ Pa

Also, outside pressure drop from Eq. (1), $\Delta P_{outside}$ = $\underline{7.314\ \text{Pa}}$

As, $\Delta P_{outside} > \Delta P_{inside}$, the assumed dimensions for design of cookstove are acceptable for natural draft of air required for operation of the cookstove.

Thus, as per the design parameters reported in Table 1, the cookstove was fabricated by the professions in a factory (Figure 4).

Fig. 4. Photograph of the factory ready community cookstove

3. Laboratory Performance of the Cookstove

3.1 Experimental Methodology

The performance of the community cookstove was tested in the laboratory according to the Bureau of Indian Standers (BIS) protocol for solid biomass cookstoves [14]. As per the procedure given in this protocol, the testing of the cookstove is conducted in two stages *viz.* i) To determine the fuel burning rate and input power of the cookstove and ii) To determine the thermal and emission performance of the cookstove. During both stages of the experimentation, each test is replicated thrice and the uncertainty analysis is conducted using the student's t-test [35].

In the present case, two kinds of experimentation are planned *viz.* stove without insulation and stove with proper insulation of alumina fibre. This will help us in the estimation of the effect of insulation on the thermal and emission performance of the cookstove.

3.1.1 To determine fuel burning capacity and input power of the cookstove

In this method, the cookstove is supplied with fuel for about 30 minutes and the mass of fuel burnt during this period (m_{f1}) is recorded. The total amount of fuel burnt for one hour (m_f) is twice of the fuel burnt during the half hour test ($m_f = 2 \times m_{f1}$)). Heat input into the cookstove (H_{in}) of the cookstove is the product of total fuel burnt in one hour to the lower calorific value (LCV) of the biomass fuel.

$$H_{in} \text{ (in kJ)} = m_f \text{ (in kg)} \times LCV \text{ (in kJ/kg)} \quad (28)$$

3.1.2 To determine thermal and emission performance of the cookstove

The BIS protocol recommends for a constant power one hour laboratory test on biomass cookstove [14]. Following procedure is used to conduct laboratory test on the community cookstove

i. The total mass of biomass fuel required for the laboratory test on cookstove is determined from the first stage test i.e., fuel burning capacity (m_f). This biomass fuel is divided equally into 10 parts. Initially (at time t = 0), the first batch i.e., 0.1 m_f of fuel is fed into the cookstove, after a duration of 6 minutes next batch of fuel (0.1 m_f) is fed into the cookstove. This process is repeated till the last batch of fuel fed into the cookstove at t = 54th minute. The test end at time t = 60 minutes i.e., when complete combustion of the fuel takes place.

ii. Depending on the fuel burning rate of the cookstove, size of aluminum pot and the mass of water (m_w) in the pot is selected from the chart given in the document of BIS protocol [14]. Let m_p be the mass of empty pot with lid. Two to three aluminum pots with the designated quantity of water are kept ready during the test. Temperature of water at ambient conditions (T_{w1}) is recorded.

iii. As the first lot of the fuel starts burning, the first aluminum pots with the designated quantity of water (m_w) are kept on the stove. The water gets heated by absorbing heat due to combustion of biomass fuel till it reaches 95^{o}C. This pot is replaced by another pot of same size and filled with same quantity of water. The water in the second pot is also heated till it reaches T_{w2} = 95^{o}C and replaced by new pot with water. This process is repeated till the test ends i.e., 60 minutes. In this case the last pot might not reach 95^{o}C. Number of pots used (n_p) and final temperature of water in the last pot (T_{w3}) is noted for calculation of efficiency of the cookstove.

iv. Fire wood with *LCV* of 16000 kJ/kg, having size of 30 mm × 30 mm × 50 mm was used as biomass fuel for the tests conducted in laboratory.

v. Following relation is used to calculate thermal efficiency of the cookstove

Hout = Heat output of the stove in kJ

$$= [(n_p-1) \times (m_w \times Cp_w + m_p \times Cp_p) \times (95-T_{w1})] + [(m_w \times Cp_w + m_p \times Cp_p) \times (T_{w3} - T_{w1})] \quad (29)$$

where, *Cpw* and *Cpp*: Specific heats of water (4.186 kJ/kg/°C) and aluminum (0.896 kJ/kg/°C) respectively.

$$\text{Thermal efficiency of the cookstove, } \eta\ (\%) = \frac{H_{out}}{H_{in}} \times 100 \quad (30)$$

$$\text{Input power of the cookstove, } P\ (\text{kW}) = H_{in}/3600 \quad (31)$$

3.2 Results and Discussion

Water boiling tests were performed on the cookstove in laboratory, using BIS protocol with and without insulation on its outer body. Alumina fiber blanket of 25 mm thickness was used as an insulating material to avoid heat loss by convection and radiation from outer body and pot skirt of the cookstove. Each test, with and without insulation, was repeated thrice. The uncertainty analysis was conducted at 95% confidence level (CL) according to student's t-test using following relations

Standard deviation,

$$s = \sqrt{\frac{\sum_{i-1}^{n}(X_i-\bar{X})^2}{n-1}} \text{ and uncertainty, } u = (t \times s)/(n)^{1/2} \quad (32)$$

where, for three replicates of the tests i.e., at n = 3, from t-table, at 95% CL, t = 4.303. The other symbols have usual meaning as reported by Navidi [36].

For a natural draft cookstove, BIS recommends minimum efficiency of 25% [14]. The average efficiency of the cookstove without and with insulation was found to be 37.3% and 42.6% respectively. That is, there was an increase in efficiency by about 5.3% due to the provision of insulation on the body of the cookstove (Figure 5). Without insulation, the whole outer body of the cookstove and the pot skirt is exposed to the ambient air causing convective and radiative heat losses. Most of these heat losses are avoided due to alumina fibre blanket insulation of 25 mm thickness. It also provides safety also to the operator as the outer body remains at near ambient temperature avoiding accidental burns while working with the cookstove. The efficiency of the cookstove with and without insulation was found to be well above the BIS limit of 25% for natural draft metal biomass cookstoves.

(a) (b)

Fig. 5. Images of the cookstove during laboratory tests, (a) cookstove without insulation, (b) cookstove with insulation

During both types of tests on the cookstove, input (fire) power was found to be of the order of 17 kW when all main air holes on the outer body were open. The stove was designed for 10 kW input power but the actual input power was 170% higher than the design power. While designing the cookstove, it was assumed that the total air required for combustion of the fuel will enter only through the main air holes and entry of the air through the fuel feeding port was not taken into consideration. But in actual case, it was found that a lot of air enters into the combustion chamber through fuel feeding port also. This causes an increase in fuel burning rate which results in higher input power of the cookstove than the design power. The use of a sliding door on the fuel feeding port will control the amount of air entering the combustion chamber resulting in control of the input power of the cookstove near design power. Table 2 reports the results obtained for the water boiling tests conducted on the cookstove in laboratory.

Table 2
Results of laboratory tests on the cookstove

Parameters	Symbol	Without Insulation			With Insulation		
		Test 1	Test 2	Test 3	Test 1	Test 2	Test 3
Mass of water in pot (kg)	m_w	40.00	40.00	40.00	40.00	40.00	40.00
Mass of vessel with lid (kg)	m_p	3.26	3.26	3.26	3.26	3.26	3.26
Mass of solid fuel consumed	m_f	3.89	3.96	3.94	3.90	3.85	3.86
Initial temp. of water (^oC)	T_{w1}	23.00	23.00	24.00	20.00	20.50	21.00
Final temp of water in the last pot (^oC)	T_{w3}	90.00	86.00	92.00	26.50	26.50	25.50
No. of pots used	n_p	2	2	2	3	3	3
Net Heat input (kJ)	H_{in}	62240.0	63408.0	63040.0	62400.0	61600.0	61760.0
Net input power (kW)	P	17.29	17.61	17.51	17.33	17.11	17.16
Net heat output (kJ)	H_{out}	23680.67	22999.21	23680.67	26662.05	26406.50	25980.59
Net thermal efficiency (%)	η	38.05	36.27	37.56	42.73	42.87	42.07
Average thermal efficiency	η_{avg}	37.29			42.55		
Standard deviation for η	s_η	0.92			0.43		
Uncertainty@95% CL for η	u_η	2.28			1.06		
Efficiency with uncertainty (%)	$\eta_{avg} \pm u_\eta$	37.29 ± 2.28			42.55 ± 1.06		
Average Input power (kW)	P_{avg}	17.47			17.20		
Standard deviation for P	s_P	0.17			0.12		
Uncertainty@95% CL for P	u_P	0.41			0.29		
Input power with uncertainty (kW)	$P_{avg} \pm u_P$	17.5 ± 0.4			17.2 ± 0.3		

3.2.1 Effect of main air hole closing on performance of the cookstove

There are 20 main air holes on the outer body of the cookstove. To investigate the contribution of the main air holes to the overall performance of the cookstove, five conditions of main air hole closing were maintained *viz.* 0%, 25%, 50%, 75% and 100%. During each main air hole closing condition, water boiling tests were conducted according to BIS protocol [14]. Each test was replicated thrice and the uncertainties in input power and thermal efficiency were investigated using the student's t-test.

As the main air supply holes are closed, less amount of air will be available for fuel burning, resulting in a decrease in the input power of the cookstove (Figure 6(a)). With the increase in the percentage of air hole closing from 0% i.e., all air holes open to 100% i.e., all air holes closed, the average input power decreases from 17.5 kW to 7.4 kW and the That is, there was a 236% decrease in the input power of the cookstove for 100% closing of the main air holes. During each condition of air hole closing, as the entry of the air through the fuel feeding port was allowed, the operation of the cookstove was continued at a lower fuel burning rate than the normal one.

At 0, 25, 50, and 75% of air hole closing, the average thermal efficiency dropped slightly from 37.3% to 35.5% (Figure 6(b)). This drop in efficiency was within the uncertainty range and hence almost negligible. It is very important to note that the input power dropped from 17.5 kW to 12.4 kW during these tests. All these input power values are above the design input power of 10 kW. That is the stove was found to be operating efficiently when up 75% of the main air holes were closed.

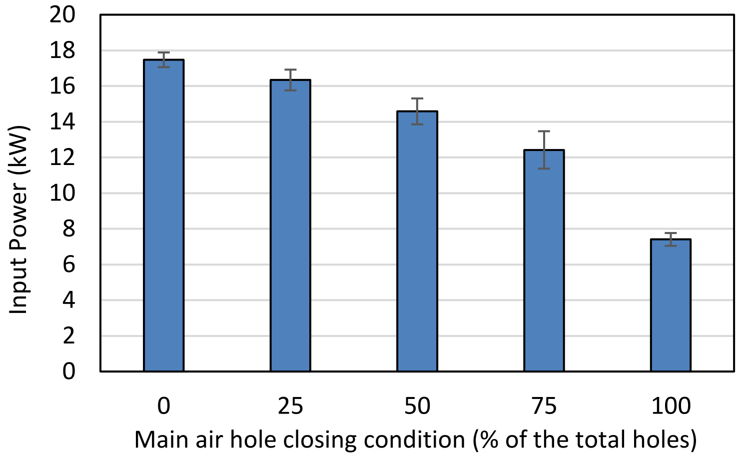

(a)

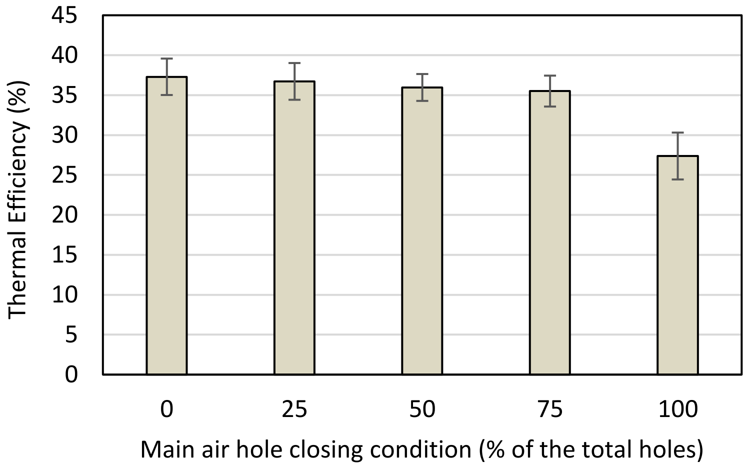

(b)

Fig. 6. Variation in (a) input power and (b) thermal efficiency at different main air hole closing conditions

The air entraining through the main air holes and through the fuel feeding port was sufficient for the efficient operation of the cookstove during the first four conditions of the cookstove. When all main air holes were closed, the only possible entry for the air was through the fuel feeding port. This might be insufficient for the efficient operation of the cookstove. Hence as 100% of main air holes were closed, the average efficiency dropped to 27% at an input power of 7.4 kW.

As discussed earlier, some of the air entering through the main air holes enters the combustion chamber as primary air which initiates the combustion process, helps the fuel in its pyrolysis and the remaining air enters at the top of the combustion chamber as a secondary air which helps the pyrolysis products in their efficient combustion.

Thus, at 100% closing of main air holes, there will be theoretically no secondary air available for efficient combustion of the pyrolysis products resulting in a sudden decrease in combustion efficiency and then the overall efficiency of the cookstove. An insufficient supply of secondary air also results in a sharp increase in emissions of carbon monoxide and unburnt hydrocarbons.

The cookstove designed for 10 kW input power was found to operate in the range of 17.5 kW to 7.4 kW i.e., with a turn down ratio (it is the ratio of maximum power to minimum power between which the cookstove can operate without interruption) of 2.4.

4. Conclusions

The present article reported a detailed procedure for design of a community cookstove using heat transfer and fluid flow considerations. Data available in literature was used at appropriate places for calculation of pressure drop in different sections of the cookstove. The cookstove was fabricated as per the design. Laboratory testing of the cookstove was conducted according to BIS protocol and analysis of data was performed [14]. Following conclusions can be drawn from the present exercise

i. It is possible to develop a combustion system such as a biomass cookstove using fundamental equations of heat transfer, fluid mechanics and the related data available in literature.
ii. The average efficiency of the cookstove was found to be 42.6% (at 17.5 kW average input power) and 37.3% (at 17.2 kW average input power) with and without insulation respectively. The efficiency of the cookstove with and without insulation was found to be well above the BIS limit of 25% for natural draft metal biomass cookstoves.
iii. The highest average efficiency of the cookstove was found to be 42.6% and 37.3% with and without insulation respectively. That is there was the improvement in efficiency by about 5.3% due to insulation.
iv. When main air holes were closed from 0% to 75%, the average efficiency and input power of the cookstove were found to be in the range of 37.3% at 17.5 kW to 35.5% at 12.4 kW. Thus, in this range of main air opening, the variation in average efficiency was within uncertainty limits though considerable variation in input power was reported.
v. The provision of primary and secondary air holes plays a very important role in the performance of a cookstove. When 100% main air holes were closed, the average efficiency of the cookstove was found to be poor (27.3%) due to no supply of secondary air to the combustion chamber of the cookstove.

It is proposed to conduct field studies on the new community cookstove at the community kitchens. Also, it is proposed to measure pollutant emissions during operation of the cookstove. Based on the suggestions from the end users, modifications will be done in the present design.

Acknowledgement
This research was not funded by any grant.

References
[1] WHO. "Household air pollution and health." *World Health Organization*. November 28, 2022.
[2] Chomcharn A. "Improved biomass cooking stoves for household use." *Royal Forest Department, Thailand*, 2022.
[3] Lepeleire, G. D., K. Krishna Prasad, P. Verhaart, and P. Visser. "A woodstove compendium." *Woodburning Stove Group, Technical University, Eindhoven, Netherlands* (1981).
[4] Mazumdar, A. *Consolidation of information: cooking stoves handbook*. Tata Energy Research Institute, 1982.
[5] Krishna Prasad, K., and P. Verhaart. "Combustion and heat transfer in small-scale woodburning devices." *TU Eindhoven. Vakgr. Transportfysica: Rapport* (1987).
[6] Kumar, Manoj, Sachin Kumar, and S. K. Tyagi. "Design, development and technological advancement in the biomass cookstoves: A review." *Renewable and Sustainable Energy Reviews* 26 (2013): 265-285. https://doi.org/10.1016/j.rser.2013.05.010
[7] Kshirsagar, Milind P., and Vilas R. Kalamkar. "A comprehensive review on biomass cookstoves and a systematic approach for modern cookstove design." *Renewable and Sustainable Energy Reviews* 30 (2014): 580-603. https://doi.org/10.1016/j.rser.2013.10.039

[8] Simon, Gregory L., Rob Bailis, Jill Baumgartner, Jasmine Hyman, and Arthur Laurent. "Current debates and future research needs in the clean cookstove sector." *Energy for Sustainable Development* 20 (2014): 49-57. https://doi.org/10.1016/j.esd.2014.02.006
[9] Sutar, Kailasnath B., Sangeeta Kohli, M. R. Ravi, and Anjan Ray. "Biomass cookstoves: A review of technical aspects." *Renewable and Sustainable Energy Reviews* 41 (2015): 1128-1166. https://doi.org/10.1016/j.rser.2014.09.003
[10] Mehetre, Sonam A., N. L. Panwar, Deepak Sharma, and Himanshu Kumar. "Improved biomass cookstoves for sustainable development: A review." *Renewable and Sustainable Energy Reviews* 73 (2017): 672-687. https://doi.org/10.1016/j.rser.2017.01.150
[11] Memon, Shebaz A., Meet S. Jaiswal, Yuvan Jain, Vaibhav Acharya, and Darshit S. Upadhyay. "A comprehensive review and a systematic approach to enhance the performance of improved cookstove (ICS)." *Journal of Thermal Analysis and Calorimetry* 141, no. 6 (2020): 2253-2263. https://doi.org/10.1007/s10973-020-09736-2
[12] Lindgren, Samantha A. "Clean cooking for all? A critical review of behavior, stakeholder engagement, and adoption for the global diffusion of improved cookstoves." *Energy Research & Social Science* 68 (2020): 101539. https://doi.org/10.1016/j.erss.2020.101539
[13] Lindgren, Samantha. "Cookstove implementation and Education for Sustainable Development: A review of the field and proposed research agenda." *Renewable and Sustainable Energy Reviews* 146 (2021): 111184. https://doi.org/10.1016/j.rser.2021.111184
[14] BIS. "Indian Standard on Portable Solid Bio-Mass Cookstove (Chulha) [First revision of IS: 13152(Part 1):1991]." *Bureau of Indian Standards, Government of India* (2013).
[15] Debajit, Palit, and Mande Sanjay. "Biomass gasifier systems for thermal applications in rural areas." *Boiling Point* 53 (2007): 17-19.
[16] Lewis, Jessica J., Vasundhara Bhojvaid, Nina Brooks, Ipsita Das, Marc A. Jeuland, Omkar Patange, and Subhrendu K. Pattanayak. "Piloting improved cookstoves in India." *Journal of Health Communication* 20, no. sup1 (2015): 28-42. https://doi.org/10.1080/10810730.2014.994243
[17] Menghwani, Vikas, Hisham Zerriffi, Puneet Dwivedi, Julian D. Marshall, Andrew Grieshop, and Rob Bailis. "Determinants of cookstoves and fuel choice among rural households in India." *EcoHealth* 16, no. 1 (2019): 21-60. https://doi.org/10.1007/s10393-018-1389-3
[18] Smokeless Cookstove Foundation. "India's Community Kitchens and Clean Cooking Nexus." *Smokeless Cookstove Foundation Report*, 2020.
[19] Robinson, Benjamin L., Mike J. Clifford, Joseph Hewitt, and Sarah Jewitt. "Cooking for communities, children and cows: Lessons learned from institutional cookstoves in Nepal." *Energy for Sustainable Development* 66 (2022): 1-11. https://doi.org/10.1016/j.esd.2021.10.012
[20] Baharuddin, Baharuddin, Janter Pangaduan Simanjuntak, Eka Daryanto, Bisrul Hapis Tambunan, Hanapi Hasan, Samsudin Anis, and Mochamad Syamsiro. "Development of a Small-Scale Electricity Generation Plant Integrated on Biomass Carbonization: Thermodynamic and Thermal Operating Parameters Study." *Journal of Advanced Research in Fluid Mechanics and Thermal Sciences* 94, no. 1 (2022): 79-95. https://doi.org/10.37934/arfmts.94.1.7995
[21] Jankaew, Nilnet, Mohd Faizal Mohideen Batcha, Arkom Palamanit, Maizirwan Mel, and Makatar Wae-hayee. "The Effects of Pressure and Temperature on Flame Characteristics of Crude Palm Oil Combustion." *Journal of Advanced Research in Fluid Mechanics and Thermal Sciences* 98, no. 2 (2022): 165-174. https://doi.org/10.37934/arfmts.98.2.165174
[22] Martin, Awaludin, P. S. Utama, Y. R. Ginting, and N. Khotimah. "Improvement of Biocoal Quality from Empty Oil Palm Fruit Bunches by Using Peat Water to Reducing Potassium Content and Torrefaction at 300°C to Increasing Heating Value." *Journal of Advanced Research in Fluid Mechanics and Thermal Sciences* 90, no. 2 (2021): 32-41. https://doi.org/10.37934/arfmts.90.2.3241
[23] Balli, Lahcen, Adil Atifi, Mohamed Hlimi, Bachir Hamri, and Youssef Achenani. "Experimental Study and Energy Optimization of a Prototype Furnace for the Pottery-Ceramic Industry." *Journal of Advanced Research in Fluid Mechanics and Thermal Sciences* 98, no. 2 (2022): 44-57. https://doi.org/10.37934/arfmts.98.2.4457
[24] Bryden, Mark, Dean Still, Peter Scott, Geoff Hoffa, Damon Ogle, Rob Bailis, and Ken Goyer. *Design principals for wood burning cook stoves*. Aprovecho Research Center, 2005.
[25] Modi, P. N., and S. M. Seth. *Hydraulics and Fluid Mechanics Including Hydraulics Machines*. Rajsons Publications Pvt. Ltd., 2019.
[26] Gudekote, Manjunatha, and Rajashekhar Choudhari. "Slip effects on peristaltic transport of Casson fluid in an inclined elastic tube with porous walls." *Journal of Advanced Research in Fluid Mechanics and Thermal Sciences* 43, no. 1 (2018): 67-80.
[27] Brady, Michael P., Kelly Banta, John Mizia, Nathan Lorenz, Donovan N. Leonard, Yukinori Yamamoto, Morgan DeFoort, and James R. Keiser. "Alloy corrosion considerations in low-cost, clean biomass cookstoves for the

developing world." *Energy for Sustainable Development* 37 (2017): 20-32. https://doi.org/10.1016/j.esd.2016.12.002
[28] MacCarty, Nordica A., and Kenneth M. Bryden. "A generalized heat-transfer model for shielded-fire household cookstoves." *Energy for Sustainable Development* 33 (2016): 96-107. https://doi.org/10.1016/j.esd.2016.03.003
[29] Kaviany, Maasoud. *Principles of heat transfer in porous media*. Springer Science & Business Media, 2012.
[30] Zube, Daniel Joseph. "Heat transfer efficiency of biomass cookstoves." *PhD diss., Colorado State University*, 2010.
[31] Bergman, Theodore L., Theodore L. Bergman, Frank P. Incropera, David P. Dewitt, and Adrienne S. Lavine. *Fundamentals of heat and mass transfer*. John Wiley & Sons, 2011.
[32] White, Frank M. *Fluid mechanics*. Tata McGraw-Hill Education, 1979.
[33] Engineers Edge. "Convection heat transfer coefficients table chart." *Engineers Edge*.
[34] Carvill, James. *Mechanical engineer's data handbook*. Butterworth-Heinemann, 1994.
[35] Montgomery, Douglas C. *Design and analysis of experiments*. John Wiley & Sons, 2017.
[36] Navidi, William Cyrus. *Statistics for engineers and scientists*. Vol. 2, no. 4. New York, NY, USA: McGraw-Hill Higher Education, 2008.